Utkal University Journal of Computing & Communications,
Vol. 1, Issue. 2 (2023) *e-ISSN:2584-203X*

Analysis of a Double Gate MOSHEMT for application in wireless communication

Swagatika Meher[1], Ananya Dastidar[1*] [0000-1111-2222-3333]

[1] Odisha University of Technology and Research, Bhubaneswar
*adastidar@outr.ac.in

Abstract: The rapid evolution of wireless communication technologies, specifically the deployment of wireless networks, demands innovative semiconductor devices to meet the stringent requirements for high-frequency operation, low power consumption, and enhanced data rates. In this context, Double-Gate Metal-Oxide-Semiconductor High-Electron-Mobility Transistors (MOSHEMTs) have emerged as a promising solution due to their unique combination of Metal-Oxide-Semiconductor Field-Effect Transistor (MOSFET) and High-Electron-Mobility Transistor (HEMT) characteristics. This paper provides a comprehensive review of the design, and performance characteristics of Double-Gate MOSHEMTs tailored for wireless applications. The inclusion of the double-gate configuration allows for improved control over the Two-Dimensional Electron Gas (2DEG) formed at the semiconductor-oxide interface, leading to enhanced electron mobility and high frequency. All simulations were conducted using the Visual TCAD 2D simulator from Cogenda.

Keywords: GaN, MOSHEMT, wireless, HfO_2, TCAD

1. Introduction

Traditional MOSFETs must be constructed with extremely short channel lengths to meet the demands of high frequency, low noise, and high power density applications[1]. This is done to ensure that most of the carriers experience the least amount of impurity scattering and that performance degradation is downplayed. These applications also imply design and performance constraints, demanding great transconductance and high saturation current, which can be accomplished with extensive doping. To get out of these restrictions, MOSHEMT devices use hetero-junctions, which are made of two distinct band-gap materials and prevent impurity scattering by confining electrons in a quantum well[2]. In MOSHEMT, AlGaN, a better alternative for a barrier material, has been used in high-frequency operation combined with the direct bandgap GaN material. Additionally, AlGaN/GaN MOSHEMT is a superb device that has undergone recent intensive investigation[3]. It has high breakdown strength, a high electron velocity in saturation, and can operate at very high frequencies with adequate performance[4]–[7]. Device performance in these kinds of HEMTs is dependent on the AlGaN layer's doping concentration, type of material layer, and layer thickness, providing flexibility in the design process.

Various MOSHEMTs have been analyzed for different applications. The analog/RF performance of AlInN/GaN underlap double gate MOSHEMT is inspected in [8]. This device is designed using Al2O3 gate dielectric with different gate lengths. Here, scaling of gate length leads to an increase in drain current, transconductance, output

✉ adastidar@outr.ac.in

conductance, and frequency but, at the expense of reduced transconductance generation factor. It also represented that a thinner barrier layer leads to improved TGF, transconductance, cutoff frequency, and maximum frequency. The DC and RF performance of MOSHEMTs made on AlGaN/GaN metal-oxide semiconductors with different gate lengths from 90 to 500 nm using MgCaO as gate dielectric[9] showed that due to reducing in short channel effect, the ON/OFF ratio increases with increasing gate length. This study also proposed that by lowering the gate leakage current while preserving strong RF performances for high-power applications, MgCaO shows promise as a dielectric for GaN MOS technology. A small-scale quantitative model based on the density of states at the oxide semiconductor interface for AlGaN/GaN MOSHEMT is proposed in [10]. They have studied the gate capacitance behavior in terms of capacitance-voltage characteristics. By varying barrier thickness as well as oxide thickness, the threshold voltage is also analyzed. The performance of a new 20 nm metal oxide semiconductor high electron mobility transistor (MOSHEMT) on a silicon substrate in the DC and RF domains [11] designed in T shape with a heavily doped source and drain region, a multi-layer cap and a very thin layer of HfO2 as gate dielectric. This work gave the most suitable device that can be used for future sub-millimeter wave applications. A novel enhancement-mode GaN MOS-HEMT with a high-κ TiO2 gate dielectric and a 10 nm T-gate length presented in [12] showed an outstanding performance at a threshold voltage of 1.07 V at VDS=5 V. As increasing in drain voltage, the RF parameters are also increasing. This enhancement mode MOSHEMT achieved a high cut-off frequency was about 524 GHz.

A hafnium silicate (HfSiOx) and Al2O3, are applied in AlGaN/GaN HEMTs as high K dielectric in [13] following post-deposition annealing at 800 °C, a plasma-enhanced atomic layer deposition method was used to create the (HfO2)/(SiO2) laminate structure on the AlGaN surface. The HfSiOx-gate HEMT had good transfer properties, including a subthreshold swing of 71 mV/decade and a strong transconductance as predicted by its dielectric value. An AlGaN/GaN-based DG MOSHEMT using Al2O3 gate dielectric in [14] shows that scaling down the gate length helps achieve a cut-off frequency of about 122.44 GHz. It is also observed that a double hump-like feature in the transconductance, which is caused by the double 2-DEG leads to improved device linearity.

MOSHEMTs are of interest in wireless communication applications due to their potential to meet the requirements for high-frequency and high-speed operations. Current wireless technology aims to deliver increased data rates, lower latency, and enhanced connectivity compared to previous generations. MOSHEMTs, especially those with advanced designs such as double-gate structures, can operate efficiently at high frequencies. This is crucial where communication often occurs in the millimeter-wave frequency range. The "HEMT" part of MOSHEMT stands for High-Electron-Mobility Transistor. This design allows for fast electron movement, making MOSHEMTs suitable for high-speed signal processing. In wireless networks, where data transfer rates are significantly higher than in previous generations, high electron mobility is essential for maintaining efficient communication. The novelty of this work lies in considering a device of sub 100 nm gate length with a high- κ dielectric as the gate oxide.

This paper focuses on presenting a HfO2 gate oxide double-gate MOSHEMT and assessing its suitability for wireless applications. The subsequent sections cover the structure of the MOSHEMT and its simulation setup in Section 2, with the model equations in Section 3, followed by the discussions of the results in Section 4, and concluding remarks in Section 5.

2. The Double Gate MOSHEMT (DG-MOSHEMT)

To enhance the device performance in terms of drain current, maximum transconductance, and maximum frequency double gate MOSHEMT is designed. Fig. 1 shows the cross-sectional view of $Al_{0.2}Ga_{0.8}N$/GaN-based double gate MOSHEMT using HfO_2 gate dielectric.

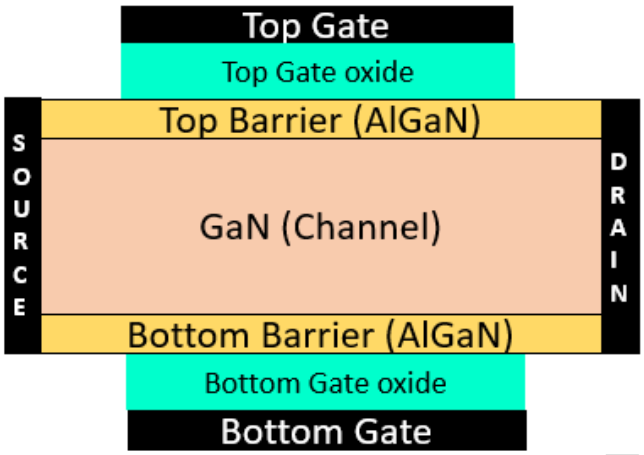

Fig. 1. Cross section of the. $Al_xGa_{1-x}N$/GaN-based Double Gate MOS-HEMT.

Top and bottom gate structures are adopted for double gate MOSHEMTs to achieve symmetrical device structure and greater control of the gate over the channel. For investing the impact of HfO_2, a device with a fixed gate length of 80 nm is used at both sides of the device. This is also a 2D gate-all-around structure. Here, only C-doped gallium nitride material is sandwiched between two barrier layers, which act as a high-resistive layer.

Table 1. Device parameters.

Parameter	**Thickness**	**Material**	**Doping**
Top Gate Length (Lg)	80 nm	$nPoly$	-
Bottom Gate Length (Lg)	80 nm	$nPoly$	-
Oxide Thickness (tox)	10 nm	HfO_2	-
Width (W)	1 μm		-
Channel Thickness (tch)	100 nm	GaN	10^{17} cm^{-3}
Barrier Thickness	50 nm	AlGaN	-
Source/ Drain	-	Al	10^{18} cm^{-3}

To inject electrons into the channel, the source and drain contacts are extended to the AlGaN barrier. Regarding the GaN channel, the simulated double-gate MOS-HEMT is symmetric. The top and bottom interfaces of AlGaN and GaN both display the polarization charge distribution. As a result, the single channel with two gates increases in 2DEG density. All the device parameters, doping concentrations, and HfO_2 oxide thickness are the same as single gate MOSHEMT shown in Table 1.

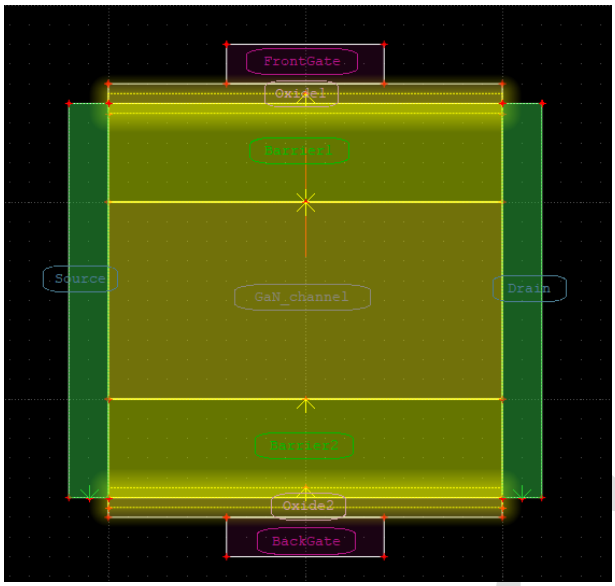

Fig. 2. Pre-Simulation model of an $Al_xGa_{1-x}N$/GaN-based Double Gate MOS-HEMT.

The pre-simulation device structure implementation in Cogenda Visual TCAD with appropriate doping is presented in Fig. 2. Circuit simulation is based on the drift-diffusion model and the SRH models have been used for carrier recombination and modeling the traps.

3. Model Equatıons

The drain current equation of an n-channel MOS-HEMT in the cut-off region is [15],

$I_D = 0$,

(1)

where, [$V_{GS} < V_T$]

The drain current equation of a n-channel MOS-HEMT in a linear region is,

$$I_{DLin} = \frac{\mu_n . C_{tot}}{2} . \frac{W}{L_G} . \left[2(V_{GS} - V_T)V_{DS} - {V_{DS}}^2 \right]$$

(2)

Where, [$V_{GS} \geq V_T \text{and} V_{DS} < V_{GS} - V_T$]

The drain current equation of a n-channel MOS-HEMT in saturation region is,

$$I_{DSat} = \frac{\mu_n . C_{tot}}{2} . \frac{W}{L_G} . (V_{GS} - V_T)^2$$

(3)

Where, [$V_{GS} \geq V_T \text{and} V_{DS} \geq V_{GS} - V_T$]

Here, C_{tot} is the oxide capacitance of the device, I_D is the drain current, W is the device width, L_G is gate length, μ_n is the electron mobility, V_{GS} is the gate to source voltage while V_{DS} is a drain to source voltage and V_T is the threshold voltage. Oxide Capacitance of the device near the top and the bottom is,

$$C_{ox,top} = C_{ox,bot} = \frac{\varepsilon_{ox}}{T_{ox}} = \frac{\varepsilon_r . \epsilon_0}{T_{ox}}$$

(4)

Since both the top and bottom oxide capacitance are in series with each other the total oxide capacitance can be

expressed as

$$C_{ox,tot} = \frac{C_{ox,top}C_{ox,bot}}{C_{ox,top}+C_{ox,bot}} \quad (5)$$

Where ε_r= relative permittivity or dielectric persistent of high-K dielectric material, ε_0 is the constant permittivity of 8.854×10^{-12} F/m and t_{ox} is the thickness of the oxide under the gate. The trans-conductance (g_m), and cut-off frequency (f_T) are ultimate crucial factors in terms of high-speed applications.

The fraction of the variation in I_D to the change in V_{GS} with steady V_{DS} is called gate transconductance (g_m). The numerical equations have been used to measure trans-conductance are as follows:

$g_m = \frac{\partial I_D}{\partial V_{GS}}$, Where V_{DS} is constant. (6)

Cut-off frequency or break frequency (f_T) is one of the most significant factors in determining the device's RF performance. Generally, f_T is the frequency of an input signal at which the current gain is unity.

$$f_T = \frac{g_m}{2\pi C_g} \quad (7)$$

Where, gate capacitance $C_g = C_{ox} \cdot W \cdot L$.

Equations (1)-(7) have been used for the theoretical calculation of cut-off frequency and other parameters.

4. Results and Discussions

All the simulations have been carried out using the Visual TCAD 2D simulator from Cogenda which is a GUI-based semiconductor device simulator used to perform prefab simulation of semiconductor devices for various applications.

4.1. Two-dimensional Electron Gas

Fig 3 shows the formation of two 2DEGs in the double gate MOSHEMT that translates to improved mobility. At the hetero-interface of the MOSHEMT, there is a discontinuity in both the conduction and valence bands. From a highly doped layer to an undoped layer, electrons diffuse. The electrons are confined in the channel's quantum well, which is about triangular. Due to the availability of states with lower energy, carriers originating from their parent dopants in the wide-gap material transfer to the narrow-gap material. Band bending happens because of charge transfer. At the interface between the two semiconductors, a free electron gas is generated in the narrow-gap material.

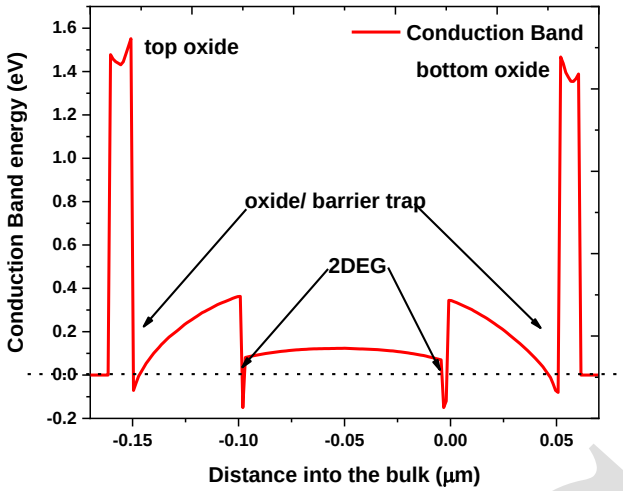

Fig. 3 2DEG of DG-MOSHEMT

The two oxide regions are represented by the potential barrier height. The oxide traps show a dip at the oxide/ semiconductor interface while the two barrier/ channel (AlGaN/ GaN) interface show the formation of two 2DEG layers.

4.2. Electron mobility of the double gate MOSHEMT

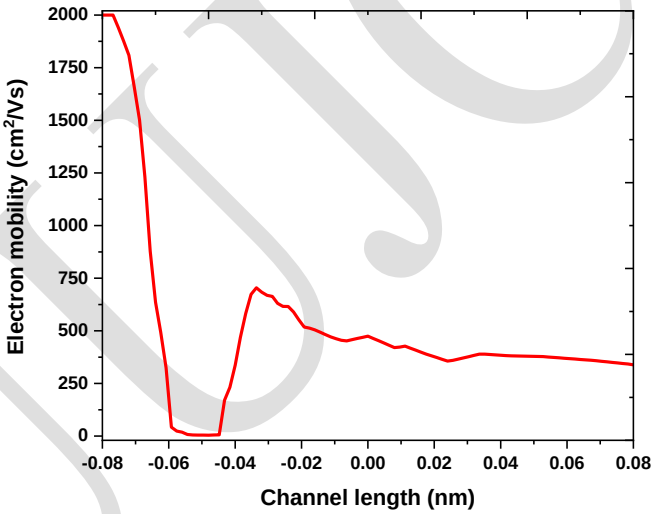

Fig. 4 Electron mobility of DG-MOSHEMT

As seen in Fig 4, near the source the two gates (top and bottom) provide excellent electrostatic control over the channel. This reduces short-channel effects and maintains a strong, well-confined 2DEG near the source upto 2000 cm^2/ Vs in this case. Low electric field near the source ensures minimal scattering and higher mobility for electrons in the 2DEG. As we move towards the drain side the high drain voltage creates a significant electric field, which reduces the effective mobility of electrons due to velocity saturation and increased scattering (e.g. interface roughness) downto to 750-500 cm^2/ Vs.

4.3. DC and Analog performance of the double gate MOSHEMT

The double-gate structure improves electrostatic control over the channel, leading to efficient 2DEG confinement and higher electron density in the channel. As a result, the device can achieve higher drain current for a given gate voltage,

making it suitable for high-power applications. Drain current and output conductance is plotted concerning drain voltages at gate voltage 3 V. Maximum drain current is observed at 4500 mA/mm and maximum output conductance is observed at 1150 mS/mm, shown in Fig. 5. Similarly, drain current and transconductance are plotted with respect to gate voltages at drain voltage 5 V. Maximum drain current is observed at 6000 mA/mm, and maximum transconductance is observed at 1500 mS/mm, shown in Fig. 6. The simulated threshold voltage is -1.4 V, which defines that the double gate device is operated in depletion mode. DG-MOSHEMTs have higher transconductance due to better control over the channel by the dual gates and high electron mobility in the 2DEG. This enhances the gain of analog circuits and improves their performance.

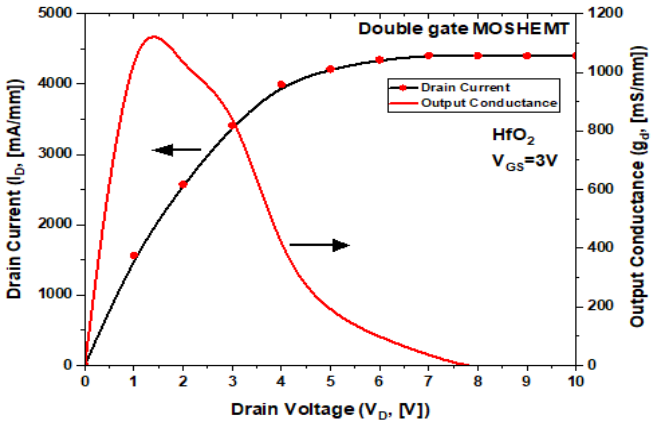

Fig. 5 (I_D -V_D) and (g_d-V_D) characteristic curves of HfO_2 dielectric DG MOSHEMT

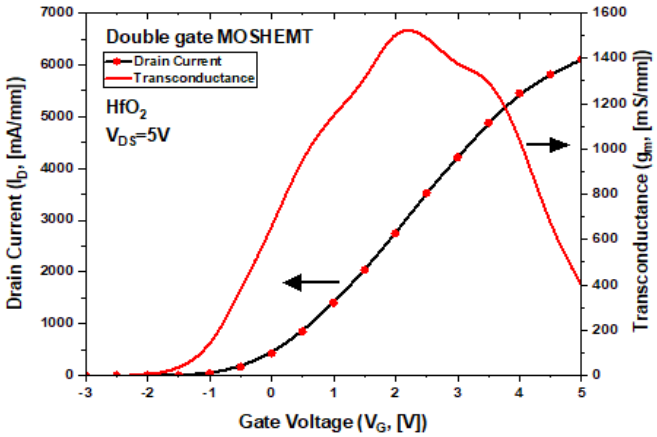

Fig. 6 (I_D –V_G) and (g_m-V_G) characteristic curves of DG MOSHEMT

The transconductance generation factor is plotted with respect to gate voltages at drain voltage 5 V. Maximum transconductance generation factor is observed at 50 V^{-1}, shown in Fig. 7. Typically, TGF between 10 V^{-1} and 5 V^{-1} variations with V_{GS} from 0.7 V to 2 V will be used for analog/ RF applications.

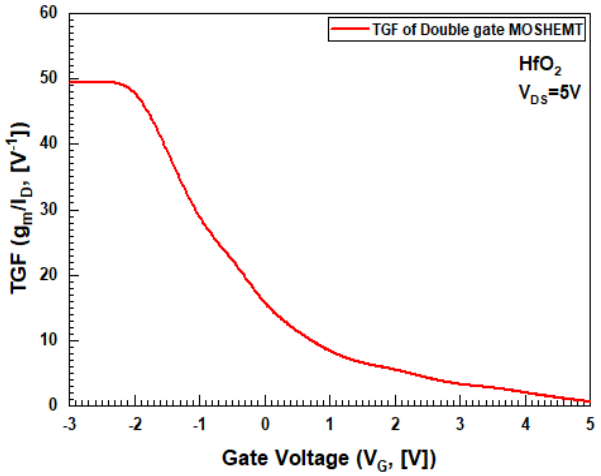

Fig. 7 TGF curve with respect to gate voltages of HfO_2 dielectric DG MOSHEMT

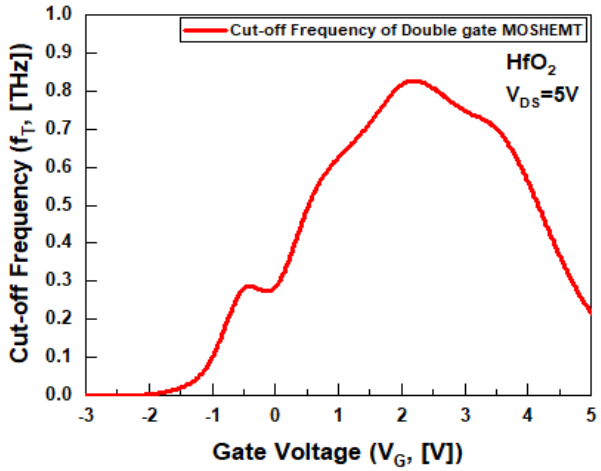

Fig. 8 Cut-off frequency curve with respect to gate voltages of HfO_2 dielectric DG MOSHEMT

The cut-off frequency is plotted with respect to gate voltages at drain voltage 5 V. Maximum cut-off frequency is observed at 0.8 THz, shown in Fig. 8. This is extracted by using the equation (7). The reduced parasitic capacitances and higher electron velocity in the channel contribute to a higher cut-off frequency, critical for high-frequency analog/RF applications.

Table 2. Device parameters of DG-MOSHEMT

Parameters	This Work	[16]	[18]
Threshold voltage (V_T)	-1.4		0.3
I_D (Max.) at V_{GS}=3V [mA/mm]	4500		
I_D (Max.) at V_{DS}=5V [mA/mm]	6000	1670	540
g_d (Max.) [mS/mm]	1150		
g_m (Max.) [mS/mm]	1500	850	160
TGF, V_{DS}=5V [V^{-1}]	50	~45	
Intrinsic gain (A_V, [dB])	2.5		
f_T (Max.)	0.8 THz	137 GHz	25 GHz

Double gate MOSHEMTs offer superior gate control, supressed SCE, higher transconductance, higher break down voltage, lower SS, and higher frequency performance over its single gate counterpart. The high cut-off frequency as shown in Table 2 and in comparison, with existing literature, suggests that the device can be used in domains based

on high frequency as well as high-speed communications. This establishes the promise of the dual gate MOSHEMT device for wireless communication applications.

4.4. Applications and Limitations

Double-Gate MOSHEMTs are highly suitable for wireless applications like 5G, IoT, and radar systems due to their exceptional high-frequency and low-noise performance. The dual-gate design ensures superior electrostatic control, leading to higher transconductance, cutoff frequency, and power gain, essential for efficient RF amplifiers and transceivers. Additionally, their low output conductance and enhanced linearity improve signal fidelity, critical for 5G and radar. The device's high breakdown voltage and thermal stability enable reliable performance under high-power conditions, while its low noise figure enhances IoT sensor sensitivity. However, fabrication complexity and thermal management remain challenges for large-scale deployment.

5. Conclusıon

This paper aims to contribute to the understanding of Double-Gate MOSHEMTs and their role in advancing semiconductor technology for the next generation of high-performance wireless communication applications. This paper presents a modified study of the analog/RF characteristics of the AlGaN/GaN DG MOSHEMT using the Visual TCAD tool. The dual gates enable precise tuning of the surface potential, influencing the 2DEG formation and overall device performance. The effects of high –κ dielectric on device performance have been investigated considering DC, analog, and wireless applications. With reference to RF and analog applications, the devices need to be operated in the above threshold regime. The suitable TGF value for RF/ analog performance is 5 V-1 achieved by DG MOSHEMT devices at lower gate voltage -1 V to 0 V. The double gate device is operated in depletion mode, which is superior in DC and RF performances when compared to E-mode MOSHEMTs. It is observed that the DG device has a maximum frequency of 0.8 THz, which is undoubtedly the most suitable candidate for sub-millimeter and terahertz wave applications like wireless communication, satellite communication, and 5G communication. Hence, the present DG MOSHEMT using HfO2 gate dielectric leads to further improvement in TGF and intrinsic gain as it provides superior transfer characteristics.

References

1. R. G. Arns, “The other transistor: Early history of the metal-oxide-semiconductor field-effect transistor,” Engineering Science and Education Journal, vol. 7, no. 5. Institution of Engineering and Technology, pp. 233–240, 1998, doi: 10.1049/esej:19980509.
2. F. Medjdoub, M. Van Hove, K. Cheng, D. Marcon, M. Leys, and S. Decoutere, “Novel E-Mode GaN-on-Si MOSHEMT using a selective thermal oxidation,” IEEE Electron Device Lett., vol. 31, no. 9, pp. 948–950, 2010, doi: 10.1109/LED.2010.2052014.
3. Q. Li, X. Zhou, C. W. Tang, and K. M. Lau, “High-performance inverted In 0.53Ga 0.47As MOSHEMTs on a GaAs substrate with regrown source/drain by MOCVD,” IEEE Electron Device Lett., vol. 33, no. 9, pp. 1246–1248, 2012, doi: 10.1109/LED.2012.2204431.
4. D. Meng et al., “Low leakage current and high-cutoff frequency AlGaN/GaN MOSHEMT using submicrometer-footprint thermal oxidized TiO2/NiO as Gate Dielectric,” IEEE Electron Device Lett., vol. 34, no. 6, pp. 738–740, 2013, doi: 10.1109/LED.2013.2256102.

5. A Leuther, T. Merkle, R. Weber, R. Sommer, and A. Tessmann, "THz Frequency HEMTs: Future Trends and Applications," 2019 Compd. Semicond. Week, CSW 2019 - Proc., pp. 1–2, 2019, doi: 10.1109/ICIPRM.2019.8819000.
6. BY. Chou et al., "TiO2-dielectric AlGaN/GaN/Si metal-oxide-semiconductor high electron mobility transistors by using nonvacuum ultrasonic spray pyrolysis deposition," IEEE Electron Device Lett., vol. 35, no. 11, pp. 1091–1093, 2014, doi: 10.1109/LED.2014.2354643.
7. CB. Zota, C. Convertino, M. Sousa, D. Caimi, K. Moselund, and L. Czornomaz, "High-frequency quantum well InGaAs-on-Si MOSFETs with scaled gate lengths," IEEE Electron Device Lett., vol. 40, no. 4, pp. 538–541, 2019, doi: 10.1109/LED.2019.2902519.
8. H. Pardeshi, "Analog/RF performance of AlInN/GaN underlap DG MOS-HEMT," Superlattices Microstruct., vol. 88, pp. 508–517, Dec. 2015, doi: 10.1016/j.spmi.2015.10.009.
9. H. Zhou et al., "DC and RF Performance of AlGaN/GaN/SiC MOSHEMTs with Deep Sub-Micron T-Gates and Atomic Layer Epitaxy MgCaO as Gate Dielectric," IEEE Electron Device Lett., vol. 38, no. 10, pp. 1409–1412, 2017, doi: 10.1109/LED.2017.2746338.
10. R. Swain, K. Jena, and T. R. Lenka, "Modelling of capacitance and threshold voltage for ultrathin normally-off AlGaN/GaN MOSHEMT," Pramana - J. Phys., vol. 88, no. 1, pp. 1–7, 2017, doi: 10.1007/s12043-016-1310-y.
11. J. Ajayan, T. D. Subash, and D. Kurian, "20 nm high performance novel MOSHEMT on InP substrate for future high speed low power applications," Superlattices Microstruct., vol. 109, pp. 183–193, 2017, doi: 10.1016/j.spmi.2017.05.015.
12. T. Zine-eddine, H. Zahra, and M. Zitouni, "Design and analysis of 10 nm T-gate enhancement-mode MOS-HEMT for high power microwave applications," J. Sci. Adv. Mater. Devices, vol. 4, no. 1, pp. 180–187, 2019, doi: 10.1016/j.jsamd.2019.01.001.
13. R. Ochi, E. Maeda, T. Nabatame, K. Shiozaki, T. Sato, and T. Hashizume, "Gate controllability of HfSiOx/AlGaN/GaN MOS high-electron-mobility transistor," AIP Adv., vol. 10, no. 6, 2020, doi: 10.1063/5.0012687.
14. M. Verma and A. Nandi, "Design and Analysis of AlGaN/GaN Based DG MOSHEMT for High-Frequency Application," Trans. Electr. Electron. Mater., vol. 21, no. 4, pp. 427–435, 2020, doi: 10.1007/s42341-020-00196-x.
15. N. DasGupta and A. DasGupta, "An analytical expression for sheet carrier concentration vs gate voltage for HEMT modelling," Solid State Electron., vol. 36, no. 2, pp. 201–203, 1993, doi: 10.1016/0038-1101(93)90140-L.
16. M. Vadizadeh, M. Fallahnejad, M. Shaveisi, R. Ejlali, and F. Bajelan, "Double Gate Double-Channel AlGaN/GaN MOS HEMT and its Applications to LNA with Sub-1 dB Noise Figure," Silicon, vol. 15, no. 2, pp. 1093–1103, 2023, doi: 10.1007/s12633-022-02083-x.
17. D. K. Panda and T. R. Lenka, "Oxide thickness dependent compact model of channel noise for E-mode AlGaN/GaN MOS-HEMT," AEU - Int. J. Electron. Commun., vol. 82, pp. 467–473, Dec. 2017, doi: 10.1016/j.aeue.2017.09.025.
18. Panda, Deepak Kumar, Rajan Singh, Trupti Ranjan Lenka, Thi Tan Pham, Ravi Teja Velpula, Barsha Jain, Ha Quoc Thang Bui, and Hieu Pham Trung Nguyen. "Single and double-gate based AlGaN/GaN MOS-HEMTs for the design of low-noise amplifiers: a comparative study." IET Circuits, Devices & Systems 14, no. 7 (2020): 1018-1025.